LINKS IN ORTHOPLICIAL APOLLONIAN PACKINGS

Jorge Luis RAMIREZ ALFONSIN, Ivan Rasskin

LINKS IN ORTHOPLICIAL APOLLONIAN PACKINGS

JORGE L. RAMÍREZ ALFONSÍN† AND IVÁN RASSKIN‡

Abstract. In this paper, we introduce a connection between Apollonian packings and links. We present new representations of links embedded in the tangency graph of orthoplicial Apollonian packings and show that any algebraic link can be projected onto the tangency graph of a cubic Apollonian packing. We use these representations to improve the upper bound on the ball number of an infinite family of alternating algebraic links, to reinterpret the correspondence of rational tangles and rational numbers, and to find primitive solutions of the Diophantine equation $x^4 + y^4 + z^4 = 2t^2$.

1. Introduction

Apollonian packings and their generalizations appear in many different fields of science: in the modelling of granular systems [AM95], fluid emulsions [Kwo+20], in number theory [Gra+03], etc. In this paper, we push further the applications of Apollonian packings into the novel direction of knot theory by introducing new representations of links based on a generalization of the classic Apollonian packing.

1.1. **Main results.** We begin by proving that any link can be realized in the tangency graph of any *orthoplicial* Apollonian packing (Theorem 3.1). We then focus our attention to algebraic links and show that any algebraic link can be regularly projected onto the tangency graph of a *cubic* Apollonian packing (Theorem 4.1). The diagrams arising from the latter construction, called *orthocubic representations*, have the following interesting applications.

1.1.1. *Ball number.* A *necklace representation* of a link L is a sphere packing containing a collection of disjoint cycles in its tangency graph realizing L. Necklace representations have been used for the study of the volume of hyperbolic 3-manifolds [Gab+21]. The *ball number* of L, denoted by $\mathsf{ball}(L)$, is defined as the minimum number of spheres needed to construct a necklace representation of L. It is known that $\mathsf{ball}(2_1^2) = 8$ and $9 \leq \mathsf{ball}(3_1) \leq 12$ [Mae07], where 2_1^2 denotes the Hopf link and 3_1 the trefoil knot. Nowadays, the Hopf link remains the only link such that its ball number is known. In [RR21b], the authors gave a constructive proof showing that for every non-trivial and non-splittable link L, $\mathsf{ball}(L) \leq 5\mathsf{cr}(L)$ and put forward the following.

Conjecture 1. *For any nontrivial and nonsplittable link L, $\mathsf{ball}(L) \leq 4\mathsf{cr}(L)$. Moreover, the equality holds if L is alternating.*

Orthocubic representations allow us to show the validity of the inequality in the Conjecture 1 for an infinite family of alternating algebraic links (Theorem 4.2), containing the family of rational links, alternating Pretzel links or, more generally, alternating Montesinos links (see Figure 1).

2010 *Mathematics Subject Classification.* 52C26, 57K10, 11D72.

Key words and phrases. Apollonian sphere packings, Ball number, Knots, Links, Diophantine equations.

† Partially supported by grant IEA-CNRS

‡ Supported by the Austrian Science Fund (FWF), projects F-5503 and P-34763.

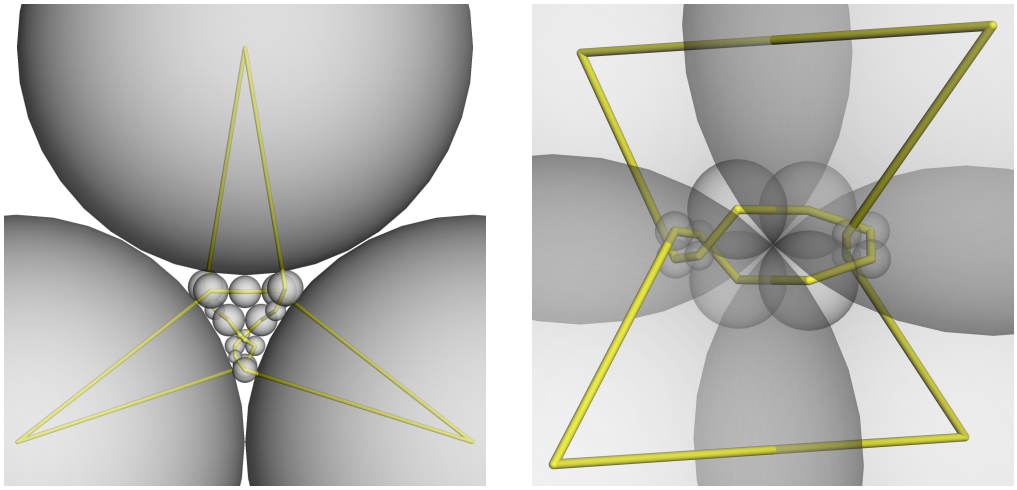

FIGURE 1. (Left) A necklace representation of the "Figure-Eight" knot 4_1 obtained by the method of [RR21b] with 20 spheres, (right) an orthocubic representation of the same knot with 16 spheres.

1.1.2. *A new visualization of the slope of rational tangles.* It is well-known that rational tangles are in correspondence to $\mathbb{Q} \cup \{\infty\}$. Orthocubic representations allow us to reinterpret this correspondence. Indeed, we show that the *slope* of rational tangle, i.e. the corresponding rational number, can be obtained from the coordinates of the intersection of an orthocubic representation of the rational tangle with a certain circle in a cubic circle packing (Theorem 5.1).

1.1.3. *Primitive solutions of a Diophantine equation.* By combining the coordinates of the intersection point described above with the Lorentz model of the space of spheres, we shall find infinitely many primitive solutions of the Diophantine equation $x^4 + y^4 + z^4 = 2t^2$ (Corollary 5.1).

1.2. **Organization.** The paper is organized as follows. In section 2, we present the background on polytopal Apollonian packings and rational tangles needed throughout the paper. In section 3, we show that every link can be embedded in the 1-skeleton of several polytopal Apollonian packings, and discuss about the optimality of the orthoplicial case regarding the number of spheres used for the constructions. In section 4, we introduce and study the orthocubic representations of rational links and show the existence of orthocubic representations of algebraic links. Finally, in Section 5, we discuss a geometric visualization of rational tangles as well as its connection with the solutions of Diophantine equations.

1.3. **Acknowledgements.** We would like to thank Alex Kontorovich for enlightening conversations on several aspects of Apollonian packings.

2. General background

In this section, we shall review notions and definitions needed in the rest of the paper. We refer the reader to [RR21b; RR21a] for more details.

2.1. **Lorentz model of the space of spheres.** An *oriented hypersphere* (in short, *sphere*) of $\widehat{\mathbb{R}^d}$ is the image of spherical cap of $\mathbb{S}^d$ under the stereographic projection. Let $\mathbb{L}^{d+1,1}$ be the Lorentz space of dimension $d+2$, i.e. the real vector space endowed with an inner product of signature $(d+1, 1)$. It is well-known that there is a bijection between spheres and points of $\widehat{\mathbb{R}^d}$ and vectors of $\mathbb{L}^{d+1,1}$ with Lorentzian norm 1 and 0, respectively. Möbius transformations of $\widehat{\mathbb{R}^d}$ corresponds to linear maps of $\mathbb{L}^{d+1,1}$ preserving the Lorentz product and the time-direction. The *inversive coordinates* of a sphere (resp. point) are the Cartesian coordinates of the corresponding vector in $\mathbb{L}^{d+1,1}$. There are several equivalent ways (up to basis exchange) to compute the inversive coordinates. We use the Wilker's convention ([Wil81]). For a sphere (resp. half-space) b with curvature $\kappa \neq 0$ and center c (resp. $\kappa = 0$, normal vector $\widehat{n}$ and signed

distance to the origin δ) its inversive coordinates are

$$\mathbf{i}(b) = \begin{cases} \frac{\kappa}{2}(2c, \|c\|^2 - 1 - \kappa^{-2}, \|c\|^2 + 1 - \kappa^{-2})^T & \text{if } \kappa \neq 0, \\ (\widehat{n}, \delta, \delta)^T & \text{if } \kappa = 0. \end{cases} \tag{1}$$

For points $\eta \in \widehat{\mathbb{R}^d}$, the inversive coordinates are

$$\mathbf{i}(\eta) \quad = \quad \begin{cases} (2\eta, \|\eta\|^2 - 1, \|\eta\|^2 + 1)^T & \text{if } \eta \neq \infty \\ (\mathbf{0}_d, 1, 1)^T & \text{if } \eta = \infty. \end{cases} \tag{2}$$

Reciprocally, if $\mathbf{i}(\eta) = (x_1, \ldots, x_{d+2})$, then $\eta = \frac{1}{x_{d+2} - x_{d+1}}(x_1, \ldots, x_d)$. We recall that the inversive coordinates of points are *homogeneous*, in the sense that for every $\lambda \neq 0$, $\lambda\mathbf{i}(\eta)$ are valid inversive coordinates of the same point of $\widehat{\mathbb{R}^d}$ [Wil81]. Under the Wilker's convention, the matrix of the Lorentz product is the diagonal matrix $\mathbf{Q}_{d+2}$ with diagonal entries $(1, \ldots, 1, -1)$, and Möbius transformations are represented by the group of matrices

$$O^{\uparrow}_{d+1,1}(\mathbb{R}) = \{\mathbf{M} \in GL_{d+2}(\mathbb{R}) \mid \mathbf{M}^T\mathbf{Q}_{d+2}\mathbf{M} = \mathbf{Q}_{d+2} \quad \text{and} \quad \mathbf{M}_{d+2,d+2} > 0\}. \tag{3}$$

The matrix of $O^{\uparrow}_{d+1,1}(\mathbb{R})$ representing the inversion s_b through the boundary of a sphere b is given by

$$\mathbf{S}_b := \mathbf{I}_{d+2} - 2\mathbf{i}(b)^T\mathbf{i}(b)\mathbf{Q}_{d+2} \tag{4}$$

where $\mathbf{I}_{d+2}$ is the identity matrix of size $d + 2$.

2.2. **Polytopal Apollonian packings.** A *polytopal* sphere packing $\mathcal{B}_\mathcal{P}$ in dimension $d \geq 1$, is the image, up to Möbius transformations, of the *ball-arrangement projection* β of an edge-scribed $(d + 1)$-polytope $\mathcal{P}$ on $\widehat{\mathbb{R}^d}$. The mapping β sends vertices of $\mathcal{P}$ to spheres of $\mathcal{B}_\mathcal{P}$ and the tangency relations are encoded by the edges of $\mathcal{P}$. For every $1 \leq n \leq d$, there is a natural realization of the n-skeleton of $\mathcal{P}$ as a CW-complex contained in $\mathcal{B}_\mathcal{P}$, which we call the *n-skeleton* of $\mathcal{B}_\mathcal{P}$, and is made by realizing the vertices of $\mathcal{P}$ as the centers of $\mathcal{B}_\mathcal{P}$, and then, for every face f of $\mathcal{P}$, taking the convex hull of the centers corresponding to the vertices of f. The 1-skeleton of $\mathcal{B}_\mathcal{P}$ corresponds to the natural realization of the tangency graph of $\mathcal{B}_\mathcal{P}$ usually called the *carrier* of the packing [Ste05]. Every polytopal sphere packing admits a *dual arrangement* $\mathcal{B}^*_\mathcal{P}$ induced by the ball arrangement projection of the polar of $\mathcal{P}$. The *Apollonian group* $\mathsf{A}(\mathcal{B}_\mathcal{P})$ is the Klenian group generated by the inversions through the dual spheres of $\mathcal{B}_\mathcal{P}$, i.e. the spheres of $\mathcal{B}^*_\mathcal{P}$. If we add the symmetries of $\mathcal{B}_\mathcal{P}$ to the set of generators, then we obtain the *symmetrized Apollonian group* of $\mathcal{B}_\mathcal{P}$, denoted by $\mathsf{SA}(\mathcal{B}_\mathcal{P})$. When the interiors of every pair of spheres in $\mathscr{P}(\mathcal{B}_\mathcal{P}) := \mathsf{A}(\mathcal{B}_\mathcal{P}) \cdot \mathcal{B}_\mathcal{P}$ are disjoint, then we obtain an infinite sphere packing that we call *polytopal Apollonian packing*. This class of infinite sphere packings can be seen as a particular case of the *crystallographic sphere packings* introduced in [KN19], where they are called *polyhedral packings*.

Remark 1. For $d \geq 2$, every polytopal sphere packing and its endowed structures are unique up to Möbius transformations. This can be seen as a consequence of the Mostow Rigidity Theorem [KN19]. In other words, any two edge-scribed realizations of a d-polytope are connected by a Möbius transformation.

2.3. **The hyperoctahedral group.** We denoted by $\mathcal{T}^d$, $\mathcal{O}^d$ and $\mathcal{C}^d$, the analogue of the regular tetrahedron, octahedron and cube in dimension $d \geq 2$, respectively (we refer to [RR21a; Ras21] for results on polytopal sphere packings arising from these polytopes). We recall that, for every $d \geq 2$, $\mathcal{O}^d$ and $\mathcal{C}^d$ are dual from each other, while $\mathcal{T}^d$ is self-dual. Among these families of polytopes, two of them are of special relevance for this paper: the cube $\mathcal{C}^3$ and the hyperoctahedron $\mathcal{O}^4$, also called *orthoplex*. The corresponding polytopal packings induced from these two polytopes are called *cubic* packings $\mathcal{B}_{\mathcal{C}^3}$ [Sta15] and *orthoplicial* packings $\mathcal{B}_{\mathcal{O}^4}$ [Nak14]. We shall index the elements by an *antipodal labelling*, where sphere b_i and $b_{\overline{i}}$ correspond to antipodal vertices in the polytope, and we shall use the bar notation $\overline{i} := -i$. The vertices of $\mathcal{O}^d$ will be labelled by $\{1, \ldots, d, \overline{1}, \ldots, \overline{d}\}$, where the facets are the $(d-1)$-simplices with vertices $\{\pm 1, \ldots, \pm d\}$. Since facets of $\mathcal{O}^d$ corresponds to vertices of $\mathcal{C}^d$, we shall label each vertex of $\mathcal{C}^d$ by the concatenation of the labelling of the vertices in $\mathcal{O}^d$ incident to the corresponding facet. The symmetry group of $\mathcal{O}^d$ (or equivalently $\mathcal{C}^d$) is called the *hyperoctahedral group*, which corresponds to the Coxeter group B_d. Under the antipodal labelling, the hyperoctahedral group is generated by the signed permutations $r_{ij} := (ij)(\overline{ij})$.

2.4. **Apollonian sections.** An *Apollonian section* of $\mathscr{P}(\mathcal{B}_\mathcal{P})$ is a subset $\mathscr{S}(\mathcal{B}_\mathcal{P}) = \Gamma \cdot X \subset \mathscr{P}(\mathcal{B}_\mathcal{P})$ where $\Gamma < \mathsf{SA}(\mathcal{B}_\mathcal{P})$ and $X \subset \mathcal{B}_\mathcal{P}$. Two Apollonian sections $\mathscr{S}(\mathcal{B}_\mathcal{P}) = \Gamma \cdot X$ and $\mathscr{S}(\mathcal{B}_\mathcal{Q}) = \Gamma' \cdot X'$ of two different Apollonian packings are said to be *algebraically equivalent* if Γ and Γ' are isomorphic and there is an equivariant bijection $\phi : \mathscr{S}(\mathcal{B}_\mathcal{P}) \to \mathscr{S}(\mathcal{B}_\mathcal{Q})$ with respect to the actions. With this notion in the hand, the second author proved in [Ras21] that any orthoplicial Apollonian packing $\mathscr{P}(\mathcal{B}_{\mathcal{O}^4})$ contains a *tetrahedral* $\mathscr{S}_{\mathcal{T}^3}(\mathcal{B}_{\mathcal{O}^4})$, *octahedral* $\mathscr{S}_{\mathcal{O}^3}(\mathcal{B}_{\mathcal{O}^4})$ and *cubic* section $\mathscr{S}_{\mathcal{C}^3}(\mathcal{B}_{\mathcal{O}^4})$, i.e. an Apollonian section which is algebraically equivalent to a tetrahedral $\mathscr{P}(\mathcal{B}_{\mathcal{T}^3})$, octahedral $\mathscr{P}(\mathcal{B}_{\mathcal{O}^3})$ and cubic Apollonian packing $\mathscr{P}(\mathcal{B}_{\mathcal{C}^3})$, respectively. We shall use a cubic section $\mathscr{S}_{\mathcal{C}^3}(\mathcal{B}_{\mathcal{O}^4})$ as a geometric framework for the constructions introduced in section 4.

2.5. **Algebraic links.** A 2-*tangle* (in short *tangle*) is a pair $(\mathcal{U}, t)$ where $\mathcal{U}$ is a compact set of $\mathbb{R}^3$ homeomorphic to a 3-ball and t is a collection $\{\gamma_1, \gamma_2, \dots, \gamma_m\}$ of $m \geq 2$ disjoint arcs contained in $\mathcal{U}$ satisfying that γ_1 and γ_2 are open arcs whose endpoints lie on the boundary of $\mathcal{U}$, and the rest of the arcs are closed. Two tangles $(\mathcal{U}, t)$ and $(\mathcal{U}', t')$ are said to be *equivalent* if there is an isotopy of $\mathbb{R}^3$ carrying $\mathcal{U}$ to $\mathcal{U}'$, t to t' and the endpoints of $(\mathcal{U}, t)$ to the endpoints of $(\mathcal{U}', t')$. We shall denote this equivalence relation $t \simeq t'$. Up to equivalence, we may consider that the endpoints of t lie on a same plane H. A *tangle diagram* of $(\mathcal{U}, t)$ is a regular projection of t on H, together with $\mathcal{U} \cap H$ and the crossing information. If it is not required, we shall refer to a tangle $(\mathcal{U}, t)$ by t. We shall name the endpoints in a tangle diagram by the cardinal points NE, NW, SE and SW. The *elementary tangles* t_0, t_1 and t_∞ are the tangles illustrated in Figure 2.

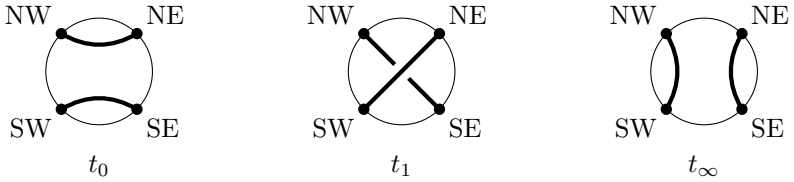

FIGURE 2. The elementary tangles.

For any two tangles t and t', we have the following operations:

(i) the *sum* $t + t'$, obtained by connecting the East endpoints of t to the West endpoints of t',

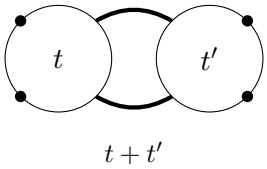

FIGURE 3. Sum of tangles.

(ii) the *mirror* $-t$: the image of t under the reflection on the plane containing the equator,
(iii) the *flip* $F(t)$: the image of t under the reflection on the plane perpendicular to the equator and passing through the endpoints SW and NE,
(iv) the *positive half-twist* $H^+ : t \mapsto t_1 + t$,
(v) the *negative half-twist* $H^- : t \mapsto -t_1 + t$.

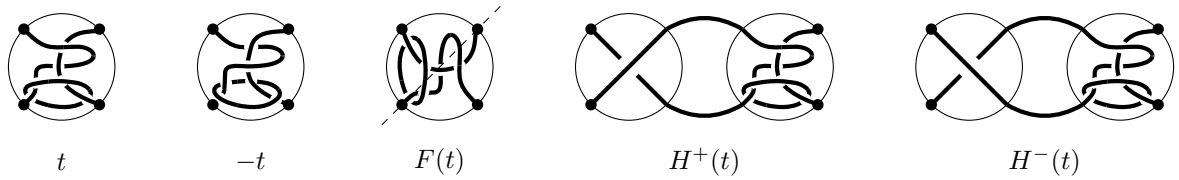

FIGURE 4. Mirror, flip and half-twist operations of tangles.

Rational tangles were introduced by Conway in his work on enumerating and classifying knots and links [Con70]. For a given sequence of integers $a_1, \ldots, a_n$ all non-zero except maybe a_1, we denote by $t(a_1, \cdots, a_n)$ the *rational tangle* given by the following Conway's algorithm [Cro04] (see Figure 5).

$$t(a_1, \cdots, a_n) := H^{a_1} F \cdots H^{a_n} F(t_\infty). \tag{5}$$

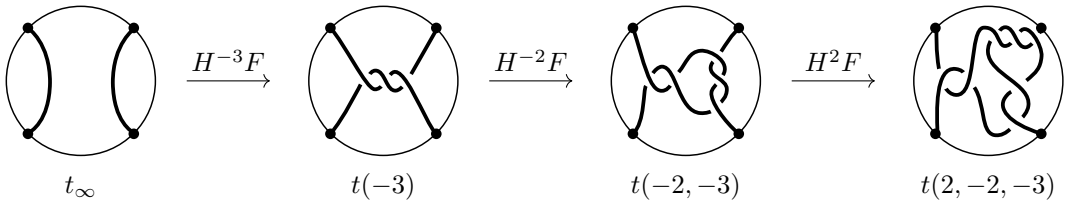

FIGURE 5. The rational tangle $t(2, -2, -3)$ obtained by the Conway's algorithm.

The *slope* of a rational tangle $t(a_1, \ldots, a_n)$ is the rational number p/q obtained by the continued fraction expansion

$$[a_1, \ldots, a_n] := a_1 + \cfrac{1}{\ddots + \frac{1}{a_n}} = \frac{p}{q}. \tag{6}$$

The origin of the name of *rational tangle* came from the connection established by the Conway's theorem [Con70], between the family of tangles produced by the Conways's algorithm and rational numbers, which states that two rational tangles are equivalent if and only if they have the same slope. We shall denote by $t_{p/q}$ the class of rational tangles with slope p/q up to isotopy. The *closure* of a tangle $(\mathcal{U}, t)$ is the link formed by joining the endpoints by two disjoint and unlinked paths at the exterior of $\mathcal{U}$. Up to equivalence, there are two possible closures, the *numerator* $N(t)$, obtained by joining the northern and the southern endpoints separately, and the *denominator* $D(t)$, obtained by joining the western and the eastern endpoints (see Figure 6).

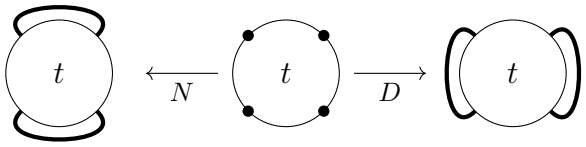

FIGURE 6. The tangle closures.

A *rational link* is the closure of a rational tangle. *Algebraic tangles* are those obtained by sums and flips of rational tangles [Ada94]. Equivalently, links which are obtained by the closure of algebraic tangles are said to be *algebraic* or *arborescent* [GT86]. Pretzel links $P(q_1, \ldots, q_n) := N(t_{1/q_1} + \cdots + t_{1/q_n})$ are a particular case of algebraic links, see Figure 7.

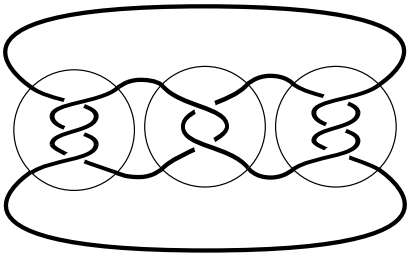

FIGURE 7. The Pretzel knot $P(3, -2, 3)$ which corresponds to the knot 8_{19} in the Alexander-Briggs notation.

3. Necklace representations in polytopal Apollonian packings

In this section, we investigate the following question: given a link L and a polytopal Apollonian sphere packing $\mathscr{P}(\mathcal{B}_{\mathcal{P}^4})$, can we find a necklace representation of L contained in $\mathscr{P}(\mathcal{B}_{\mathcal{P}^4})$? We answer positively this question for some 4-polytopes. We first have the following

Theorem 3.1. *Let L be a link and let $\mathscr{P}(\mathcal{B}_{\mathcal{O}^4})$ be an orthoplicial Apollonian sphere packing. There is a necklace representation of L contained in $\mathscr{P}(\mathcal{B}_{\mathcal{O}^4})$.*

Let us first introduce a previous notion. Let $\mathscr{P}(\mathcal{B}_{\mathcal{P}})$ be a polytopal Apollonian sphere packing, where $\mathcal{P}$ is an edge-scribed $(d+1)$-polytope. For every edge $\{i,j\} \in \mathcal{P}$, we define the *edge-figure section* of $\mathscr{P}(\mathcal{B}_{\mathcal{P}})$ as the Apollonian section $\mathscr{S}_{ij}(\mathcal{B}_{\mathcal{P}}) := \Gamma_{ij} \cdot \mathcal{B}_{\mathcal{P}}$ where Γ_{ij} is the stabilizer subgroup of the Apollonian group of $\mathcal{P}$ for $\{b_i, b_j\}$. The subgroup Γ_{ij} corresponds to a Euclidean reflection group. Indeed, we may apply an inversion to $\mathcal{B}_{\mathcal{P}}$ through a sphere centered at the tangency point of b_i and b_j mapping these two spheres into two parallel half-spaces tangent at the infinity. We then observe that every generator in Γ_{ij} must be a reflection on a hyperplane orthogonal to b_i and b_j (see Figure 9, left).

Proof of Theorem 3.1. Let $\mathcal{B}^{12}_{\mathcal{O}^4}$ the orthoplicial packing depicted in Figure 8. The edge-figure section $\mathscr{S}_{12}(\mathcal{B}^{12}_{\mathcal{O}^4}) := \Gamma_{12} \cdot \mathcal{B}^{12}_{\mathcal{O}^4}$ is generated by the action of the parabolic subgroup of the orthoplicial Apollonian group $\Gamma_{12} := \langle s_{1234}, s_{12\overline{3}4}, s_{123\overline{4}}, s_{12\overline{3}\overline{4}} \rangle$.

$\mathcal{B}^{12}_{\mathcal{O}^4}$	κ (δ if $\kappa = 0$)	c ($\widehat{n}$ if $\kappa = 0$)			$\mathbf{i}(b)^T$				
b_1	0 (1)	0	0	1	0	0	1	1	1
b_2	0 (1)	0	0	-1	0	0	-1	1	1
b_3	1	1	1	0	1	1	0	0	1
b_4	1	-1	1	0	-1	1	0	0	1
$b_{\overline{1}}$	2	0	0	$-1/2$	0	0	-1	-1	1
$b_{\overline{2}}$	2	0	0	$1/2$	0	0	1	-1	1
$b_{\overline{3}}$	1	-1	-1	0	-1	-1	0	0	1
$b_{\overline{4}}$	1	1	-1	0	1	-1	0	0	1

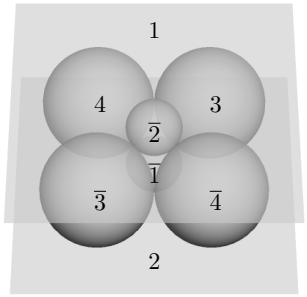

Figure 8. The orthoplicial packing $\mathcal{B}^{12}_{\mathcal{O}^4}$.

We notice that the 1-skeleton of $\mathscr{S}_{12}(\mathcal{B}^{12}_{\mathcal{O}^4})$ contains an infinite square-grid, with two vertices lying in the orthogonal line to each square and connected to every corner (see Figure 9).

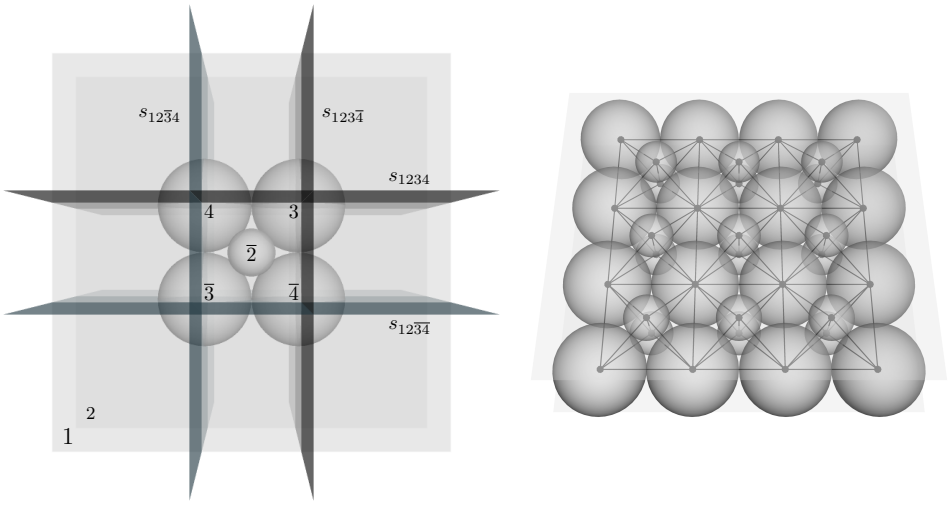

Figure 9. (Left) $\mathcal{B}^{12}_{\mathcal{O}^4}$ with the mirrors of the generators of Γ_{12}, view from above; (right) $\mathscr{S}_{12}(\mathcal{B}^{12}_{\mathcal{O}^4})$ with its 1-skeleton.

The well-known Alexander's Theorem [Ale23] implies that there is a braid γ such that its closure is isotopically equivalent to L. We can always draw a diagram of γ in a regular square-grid, where the crossings are drawn at the intersections of the diagonals of the squares, and the rest of arcs use the edges of the grid, as in Figure 10 (center). This *square-grid diagram* induces a polygonal closed path in the 1-skeleton of $\mathscr{S}_{12}(\mathcal{B}^{12}_{\mathcal{O}^4})$, as in Figure 10 (right), which gives us a necklace representation $N_L \subset \mathscr{P}(\mathcal{B}^{12}_{\mathcal{O}^4})$. Since Möbius transformations preserving the orientation are ambient isotopies of $\widehat{\mathbb{R}^3}$ then, by Remark 1, we have that there is a Möbius transformation μ carrying $\mathscr{P}(\mathcal{B}^{12}_{\mathcal{O}^4})$ to $\mathscr{P}(\mathcal{B}_{\mathcal{O}^4})$ and N_L to a necklace representation of L contained in $\mathscr{P}(\mathcal{B}_{\mathcal{O}^4})$. □

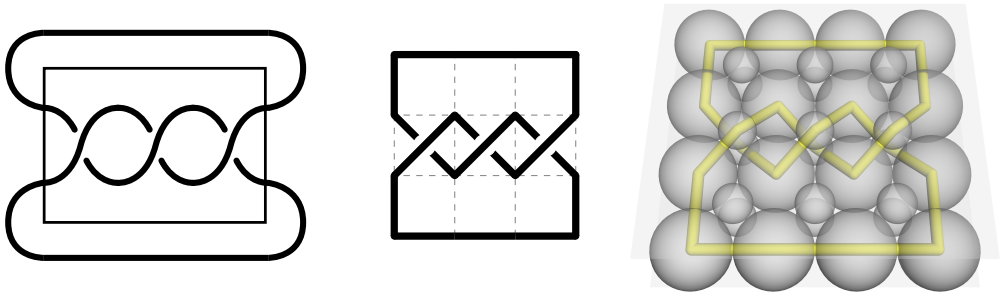

FIGURE 10. (Left) A diagram of the trefoil obtained as a closed braid; (center) a square-grid diagram of the same closed braid; (right) a necklace representation of the trefoil in $\mathscr{S}_{12}(\mathcal{B}^{12}_{\mathcal{O}^4})$.

We wonder if Theorem 3.1 can be proved without invoking Alexander's Theorem. The construction used in the proof of above can be used to show the inequality in the Conjecture 1 for 2-braid links.

Corollary 3.1. *For any 2-braid link L, we have that* $\mathsf{ball}(L) \leq 4\mathsf{cr}(L)$.

Proof. The necklace representation induced by the square-grid diagram of an alternating 2-braid with n crossings has $4n+2$ spheres (see Figure 11 (left)). For the closure, we can exchange the last 4 spheres with the two half-spaces of $\mathscr{S}_{12}(\mathcal{B}^{12}_{\mathcal{O}^4})$ (Figure 11 (right)). □

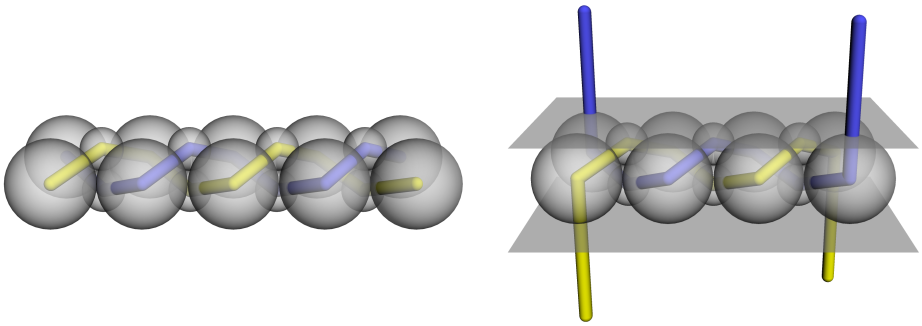

FIGURE 11. (Left) A necklace representation of the 2-braid of 4 crossings in the square-grid section, with 18 spheres; (right) a necklace representation of the closure of the 2-braid of 4 crossings, in the square-grid section, with 16 spheres.

The upper bound of Corollary 3.1 cannot be extended to n-braid links when $n \geq 3$. The main reason is that the half-spaces of the square-grid section cannot be used to close all the strands of the braid. The latter might increase the number of spheres to more than 4 times the number of crossings. A similar strategy as used in the proof of Theorem 3.1 can be employed to prove that every link admits a necklace representation in other polytopal Apollonian sphere packings $\mathscr{P}(\mathcal{B}_{\mathcal{P}^4})$. For instance, if $\mathcal{P}^4$ has a regular triangle as edge-figure, then the 1-skeleton of the edge-figure section contains a subgraph topologically equivalent to a *triangular grid*. In this case, two tangent triangles in the triangular grid made up a rhombus which can play the same role as the square in the square-grid. Indeed, if there is a

chain of spheres connecting the opposite vertices in the great diagonal of the rhombus, then we can use them to construct a crossing. It turns out that this is the case for the 4-simplex, hypercube, 24-cell or the 120-cell (see Figure 12). Although these triangular constructions produce necklace representations with more spheres that the orthoplicial one, these could be interesting for other issues like constructing 4-polytopes containing a given link in its graph [Epp14].

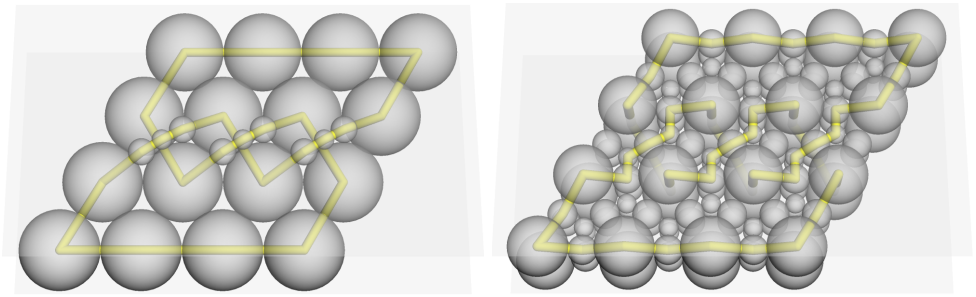

FIGURE 12. A necklace representation of the trefoil knot in $\mathscr{P}(\mathcal{B}_{\mathcal{T}^4})$ (left) and $\mathscr{P}(\mathcal{B}_{\mathcal{C}^4})$ (right).

4. Orthocubic representations of algebraic links

Let $\mathcal{B}_{\mathcal{C}^3}$ and $\mathcal{B}_{\mathcal{O}^4}$ be the cubic and the orthoplicial packing given in Figures 13 and 14, respectively. We point out that the labelling of $\mathcal{B}_{\mathcal{O}^4}$ has been given in such a way that for every $b_i \in \mathcal{B}_{\mathcal{O}^4}$, the label i is positive if and only if the third coordinate of the center of b_i is positive.

$\mathcal{B}_{\mathcal{C}^3}$	κ	c	$\mathbf{i}(b)^T$
$b_{1\overline{23}}$	$1+\sqrt{2}$	$(-1+\sqrt{2}\ \ 1\ \ -1)$	$(1\ \ -1\ \ -1\ \ \sqrt{2})$
$b_{\overline{1}2\overline{3}}$	$1+\sqrt{2}$	$(-1+\sqrt{2}\ \ -1\ \ 1)$	$(-1\ \ 1\ \ -1\ \ \sqrt{2})$
$b_{\overline{1}\overline{2}3}$	$-1+\sqrt{2}$	$(1+\sqrt{2}\ \ -1\ \ -1)$	$(-1\ \ -1\ \ 1\ \ \sqrt{2})$
b_{123}	$-1+\sqrt{2}$	$(1+\sqrt{2}\ \ 1\ \ 1)$	$(1\ \ 1\ \ 1\ \ \sqrt{2})$
$b_{\overline{1}23}$	$-1+\sqrt{2}$	$(1+\sqrt{2}\ \ -1\ \ 1)$	$(-1\ \ 1\ \ 1\ \ \sqrt{2})$
$b_{1\overline{2}3}$	$-1+\sqrt{2}$	$(1+\sqrt{2}\ \ 1\ \ -1)$	$(1\ \ -1\ \ 1\ \ \sqrt{2})$
$b_{12\overline{3}}$	$1+\sqrt{2}$	$(-1+\sqrt{2}\ \ 1\ \ 1)$	$(1\ \ 1\ \ -1\ \ \sqrt{2})$
$b_{\overline{123}}$	$1+\sqrt{2}$	$(-1+\sqrt{2}\ \ -1\ \ -1)$	$(-1\ \ -1\ \ -1\ \ \sqrt{2})$

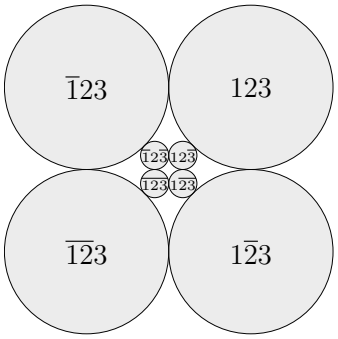

FIGURE 13. The cubic packing $\mathcal{B}_{\mathcal{C}^3}$.

$\mathcal{B}_{\mathcal{O}^4}$	κ	c	$\mathbf{i}(b)^T$
b_1	$1+1/\sqrt{2}$	$(-1+\sqrt{2}\ \ 1\ \ -1\ \ 1)$	$1/\sqrt{2}\ (1\ \ -1\ \ 1\ \ -1\ \ \sqrt{2})$
b_2	$1+1/\sqrt{2}$	$(-1+\sqrt{2}\ \ -1\ \ 1\ \ 1)$	$1/\sqrt{2}\ (-1\ \ 1\ \ 1\ \ -1\ \ \sqrt{2})$
b_3	$1-1/\sqrt{2}$	$(1+\sqrt{2}\ \ -1\ \ -1\ \ 1)$	$1/\sqrt{2}\ (-1\ \ -1\ \ 1\ \ 1\ \ \sqrt{2})$
b_4	$1-1/\sqrt{2}$	$(1+\sqrt{2}\ \ 1\ \ 1\ \ 1)$	$1/\sqrt{2}\ (1\ \ 1\ \ 1\ \ 1\ \ \sqrt{2})$
$b_{\overline{1}}$	$1-1/\sqrt{2}$	$(1+\sqrt{2}\ \ -1\ \ 1\ \ -1)$	$1/\sqrt{2}\ (-1\ \ 1\ \ -1\ \ 1\ \ \sqrt{2})$
$b_{\overline{2}}$	$1-1/\sqrt{2}$	$(1+\sqrt{2}\ \ 1\ \ -1\ \ -1)$	$1/\sqrt{2}\ (1\ \ -1\ \ -1\ \ 1\ \ \sqrt{2})$
$b_{\overline{3}}$	$1+1/\sqrt{2}$	$(-1+\sqrt{2}\ \ 1\ \ 1\ \ -1)$	$1/\sqrt{2}\ (1\ \ 1\ \ -1\ \ -1\ \ \sqrt{2})$
$b_{\overline{4}}$	$1+1/\sqrt{2}$	$(-1+\sqrt{2}\ \ -1\ \ -1\ \ -1)$	$1/\sqrt{2}\ (-1\ \ -1\ \ -1\ \ -1\ \ \sqrt{2})$

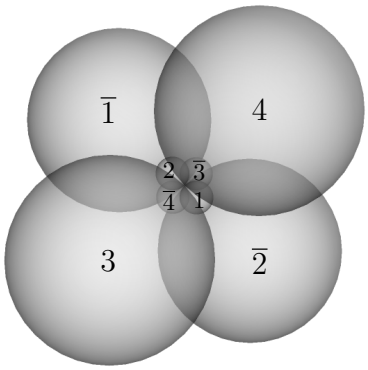

FIGURE 14. The orthoplicial packing $\mathcal{B}_{\mathcal{O}^4}$.

Let $\mathscr{S}_{\mathcal{C}^3}(\mathcal{B}_{\mathcal{O}^4}) := \Gamma_{\mathcal{C}^3} \cdot \mathcal{B}_{\mathcal{O}^4}$ be a cubic Apollonian section of $\mathscr{P}(\mathcal{B}_{\mathcal{O}^4})$, where

$$\Gamma_{\mathcal{C}^3} := \langle s_{12\overline{34}}, s_{1\overline{2}34}, s_{\overline{12}34}, s_{\overline{1}23\overline{4}}, s_{\overline{1}2\overline{3}4}, s_{1\overline{23}\overline{4}} \rangle.$$

The equivariant bijection $\phi : \mathscr{P}(\mathcal{B}_{\mathcal{C}^3}) \to \mathscr{S}_{\mathcal{C}^3}(\mathcal{B}_{\mathcal{O}^4})$ is induced by the following isomorphisms (see Figure 15).

$$\begin{array}{ccc} \mathsf{A}(\mathcal{B}_{\mathcal{C}^3}) & \longrightarrow & \Gamma_{\mathcal{C}^3} \\ s_{\pm 1} & \mapsto & s_{\pm(1\overline{2}\overline{3}4)} \\ s_{\pm 2} & \mapsto & s_{\pm(\overline{1}2\overline{3}4)} \\ s_{\pm 3} & \mapsto & s_{\pm(\overline{1}\overline{2}34)} \end{array} \qquad \begin{array}{ccc} \mathcal{B}_{\mathcal{C}^3} & \longrightarrow & \mathcal{B}_{\mathcal{O}^4} \\ b_{\pm(1\overline{2}\overline{3})} & \mapsto & b_{\pm 1} \\ b_{\pm(\overline{1}2\overline{3})} & \mapsto & b_{\pm 2} \\ b_{\pm(\overline{1}\overline{2}3)} & \mapsto & b_{\pm 3} \\ b_{\pm(123)} & \mapsto & b_{\pm 4} \end{array}$$

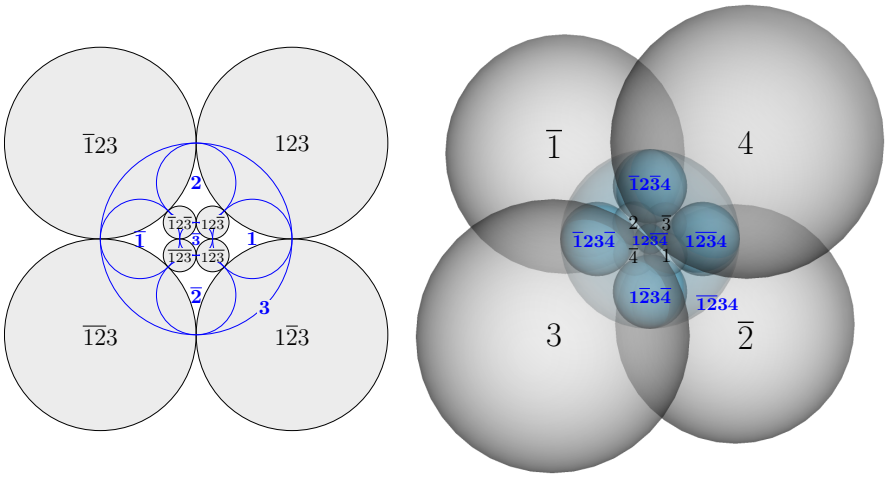

FIGURE 15. (Right) the cubic packing $\mathcal{B}_{\mathcal{C}^3}$ with its dual, (left) $\mathcal{B}_{\mathcal{O}^4}$ with the mirrors of the generators of the cubic section.

An alternative geometric way to obtain the bijection between the cubic section and cubic Apollonian packing results by taking the intersection of $\mathcal{B}_{\mathcal{O}^4}$ and its dual with the XY-plane. The relative position of the centers of the spheres in the cubic section, with respect to the XY-plane, induces a 2-coloring of the cubic Apollonian packing where two disks of same color never intersect (see Figure 16). We call this coloring the *z-coloring*. By extending the z-coloring to the vertices of the 1-skeleton of $\mathscr{P}(\mathcal{B}_{\mathcal{C}^3})$, we obtain a proper 2-coloring of the tangency graph.

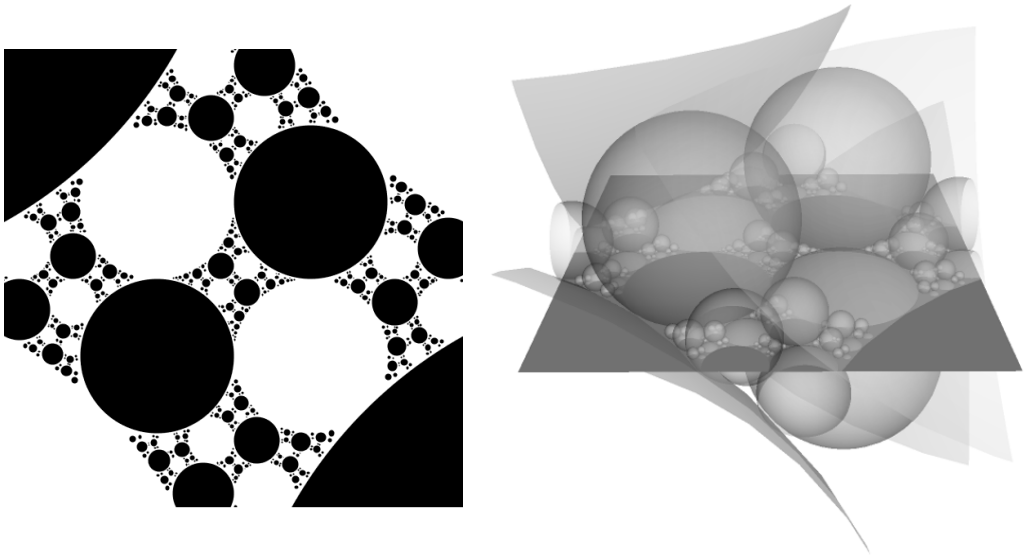

FIGURE 16. (Left) $\mathscr{P}(\mathcal{B}_{\mathcal{C}^3})$ with the z-coloring, (right) $\mathscr{S}_{\mathcal{C}^3}(\mathcal{B}_{\mathcal{O}^4})$ with the XY-plane.

On the same direction as Theorem 3.1, we present the following result allowing us to prove the inequality of the Conjecture 1 for an infinite family of alternating algebraic links (containing, in particular, 2-braid links).

Theorem 4.1. *For any algebraic link L, there is a necklace representation of L contained in $\mathscr{S}_{\mathcal{C}^3}(\mathcal{B}_{\mathcal{O}^4})$.*

4.1. **Orthocubic shifts.** Let $\mathcal{B}_{\mathcal{O}^3}$ be the octahedral packing which is the dual arrangement of the cubic packing $\mathcal{B}_{\mathcal{C}^3}$. The former can be also obtained by intersecting the dual arrangement of $\mathcal{B}_{\mathcal{O}^4}$ with the XY-plane. Let us consider the symmetries $r_{12}, r_{13}, r_{23}, r_{1\overline{3}}, r_{2\overline{3}}, r_{3\overline{3}}$, of $\mathcal{B}_{\mathcal{O}^3}$. By duality, these are also symmetries of $\mathcal{B}_{\mathcal{C}^3}$. We recall that r_{ij} denotes the signed permutation $(ij)(\overline{ij})$. In the octahedral packing $\mathcal{B}_{\mathcal{O}^3}$, we have that r_{12} corresponds to the reflection on the line $\{x = y\}$, $r_{\pm 13}$ is the inversion through the circle centered at $(\pm 1, 0)$ and radius $\sqrt{2}$, and $r_{3\overline{3}}$ is the inversion through the unit circle centered at the origin (see Figure 17).

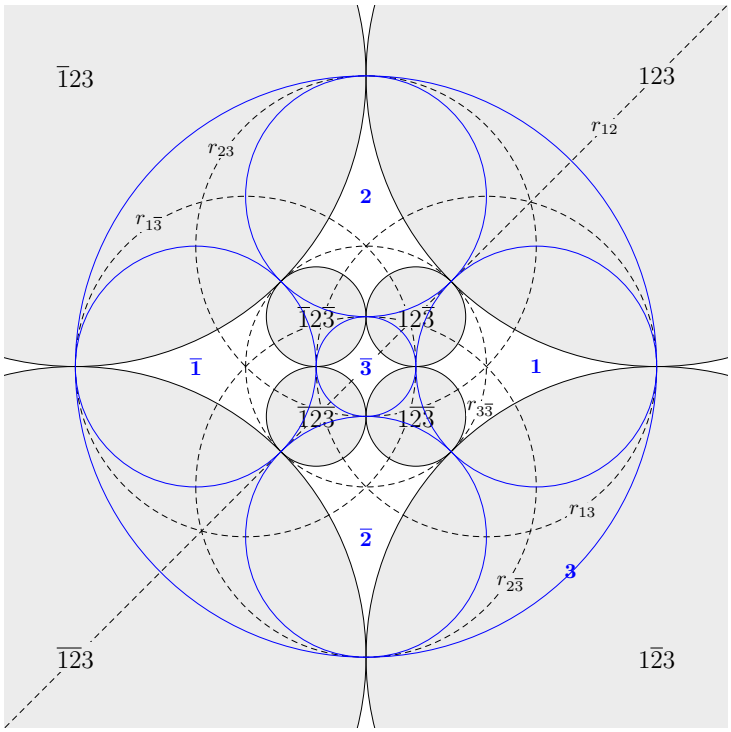

FIGURE 17. $\mathcal{B}_{\mathcal{C}^3}$ with the mirrors of the generators of the cubic shifts.

We define the *cubic shifts* as the following six elements belonging to the symmetrized Apollonian group of $\mathcal{B}_{\mathcal{C}^3}$

$$\mu_i := s_i r_{i3} \qquad \text{for every } i \in \{\pm 1, \pm 2, -3\} \qquad \text{and} \qquad \mu_3 := s_3 r_{3\overline{3}}. \tag{7}$$

In Figure 18, we show the action of the cubical shifts on the 1-skeleton of $\mathcal{B}_{\mathcal{C}^3}$ with the z-coloring. We notice that $\mu_{\pm 1}$ and $\mu_{\pm 2}$ (resp. $\mu_{\pm 3}$) preserves (resp. reverses) the z-coloring. The bijection $\phi : \mathcal{B}_{\mathcal{C}^3} \to \mathcal{B}_{\mathcal{O}^4}$ induces the following morphisms:

$$\begin{array}{rccc}
\phi: & \mathsf{Sym}(\mathcal{B}_{\mathcal{C}^3}) & \longrightarrow & \mathsf{Sym}(\mathcal{B}_{\mathcal{O}^4}) \\
& r_{12} & \longmapsto & r_{12} \\
& r_{13} & \longmapsto & r_{13} \\
& r_{23} & \longmapsto & r_{23} \\
& r_{\overline{1}3} & \longmapsto & r_{24} \\
& r_{\overline{2}3} & \longmapsto & r_{14} \\
& r_{\overline{3}3} & \longmapsto & r_{\overline{1}2} r_{\overline{3}4}
\end{array}
\qquad
\begin{array}{rccc}
\phi: & \mathsf{SA}(\mathcal{B}_{\mathcal{C}^3}) & \longrightarrow & \mathsf{SA}(\mathcal{B}_{\mathcal{O}^4}) \\
& \mu_1 & \longmapsto & s_{1\overline{2}\overline{3}4}\, r_{13} \\
& \mu_{-1} & \longmapsto & s_{\overline{1}2\overline{3}\overline{4}}\, r_{24} \\
& \mu_2 & \longmapsto & s_{\overline{1}2\overline{3}4}\, r_{23} \\
& \mu_{-2} & \longmapsto & s_{\overline{1}\overline{2}34}\, r_{14} \\
& \mu_3 & \longmapsto & s_{\overline{1}\overline{2}34}\, r_{\overline{1}2} r_{\overline{3}4} \\
& \mu_{-3} & \longmapsto & s_{12\overline{3}\overline{4}}\, r_{\overline{1}2} r_{\overline{3}4}
\end{array}$$

For every $i = \pm 1, \pm 2, \pm 3$, we call the elements $\phi(\mu_i) \in \mathsf{SA}(\mathcal{B}_{\mathcal{O}^4})$ the *orthocubic shifts*.

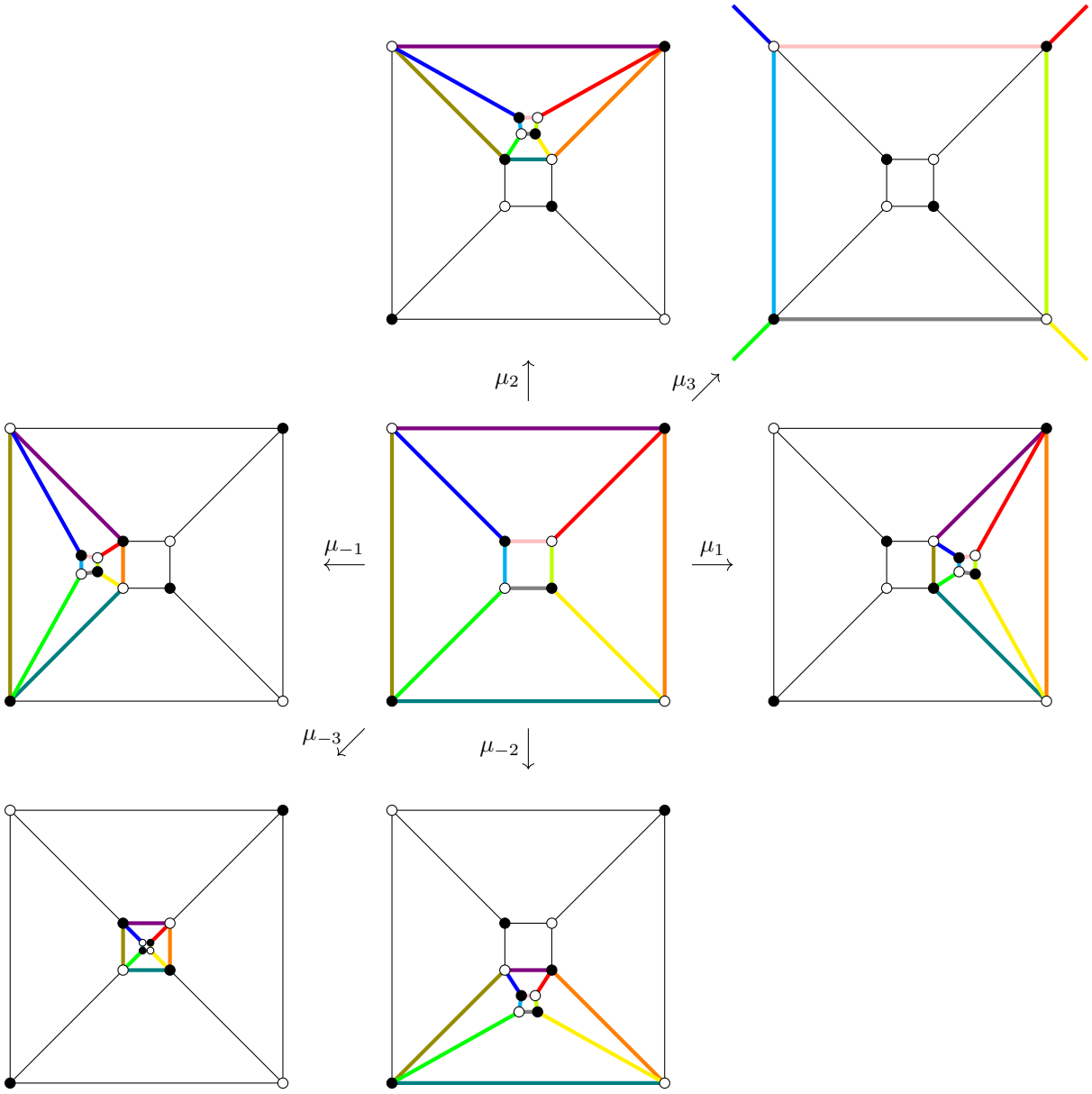

FIGURE 18. The action of the cubic shifts on the 1-skeleton of $\mathcal{B}_{\mathcal{C}^3}$ with the z-coloring.

4.2. **Orthocubic coordinates.** The cubic Apollonian packing $\mathscr{P}(\mathcal{B}_{\mathcal{C}^3})$ can be seen as a Coxeter system (W, S) where $W = \mathsf{A}(\mathcal{B}_{\mathcal{C}^3})$ and system of generators $S = \{s_{\pm 1}, s_{\pm 2}, s_{\pm 3}\}$. Its Coxeter graph is the graph of the cube with ∞ label at each edge. Therefore, the reduced words of (W, S) are the words without consecutive repeated letters. We have that for each $b \in \mathscr{S}_{\mathcal{C}^3}(\mathcal{B}_{\mathcal{O}^4})$, there is a reduce word of $w = s_{j_1} \cdots s_{j_n}$ and an element $b_i \in \mathcal{B}_{\mathcal{C}^3}$ such that $b = w \cdot b_i$. The *depth* of b is the minimal length of w in terms of the generators. By combining the reduced words of (W, S) with the bijection $\phi : \mathscr{P}(\mathcal{B}_{\mathcal{C}^3}) \to \mathscr{S}_{\mathcal{C}^3}(\mathcal{B}_{\mathcal{O}^4})$ we can give a coordinate system to the spheres is the cubic section. We define the *orthocubic coordinates* of every $b \in \mathscr{S}_{\mathcal{C}^3}(\mathcal{B}_{\mathcal{O}^4})$ as the label

$$i_{j_1 \cdots j_n} := \phi(s_{j_1}) \cdots \phi(s_{j_n}) \cdot b_i = b \tag{8}$$

where $i \in \{\pm 1, \pm 2, \pm 3, \pm 4\}$ and $j_l \in \{\pm 1, \pm 2, \pm 3\}$. In Figure 19, we show the orthocubic coordinates of the elements of $\mathscr{S}_{\mathcal{C}^3}(\mathcal{B}_{\mathcal{O}^4})$ with depth ≤ 1.

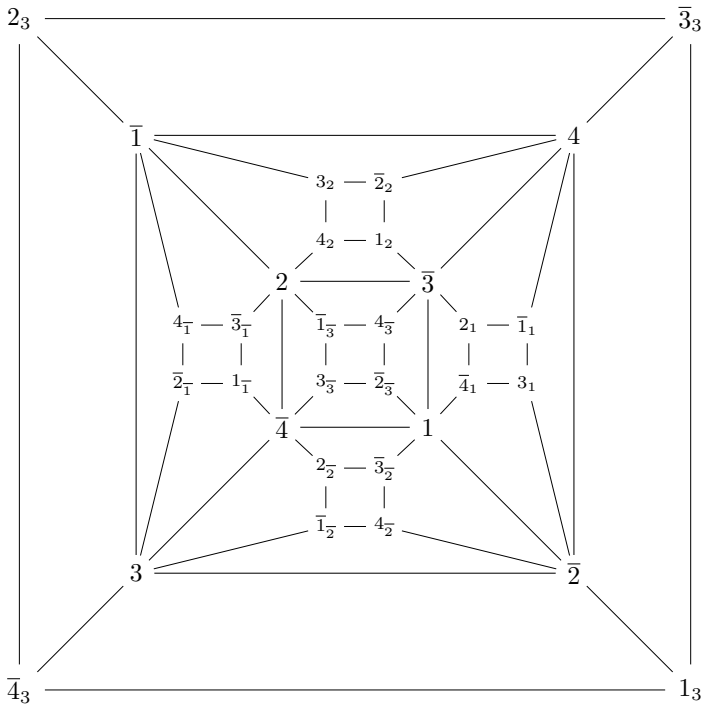

FIGURE 19. The orthocubic coordinates of the elements of $\mathscr{S}_{\mathcal{C}^3}(\mathcal{B}_{\mathcal{O}^4})$ of depth≤ 1.

4.3. **Orthocubic representations.** We define an *orthocubic path* γ as a polygonal curve in the 1-skeleton of $\mathscr{S}_{\mathcal{C}^3}(\mathcal{B}_{\mathcal{O}^4})$. A *cubic diagram* of γ will be its orthogonal projection on the XY-plane. The orthogonal projection of the 1-skeleton of $\mathscr{S}_{\mathcal{C}^3}(\mathcal{B}_{\mathcal{O}^4})$ on the XY-plane is the 1-skeleton of $\mathscr{P}(\mathcal{B}_{\mathcal{C}^3})$ plus the diagonal edges of each square-face, which join two vertices of same color under the z-coloring. The crossings of any cubic diagram are obtained by the intersection of the two diagonal edges of a same square-face. With the information given by the z-coloring, the over/under crossing information can be deduced from the color of the vertices of the diagonal edges (black=over/white=under). We define an *orthocubic representation* of a link L as a collection of disjoint closed orthocubic paths isotopically equivalent to L. Every orthocubic representation induces a necklace representation in $\mathscr{S}_{\mathcal{C}^3}(\mathcal{B}_{\mathcal{O}^4})$. In Figure 20, we show an orthocubic representation of the trefoil knot, and its corresponding cubic diagram.

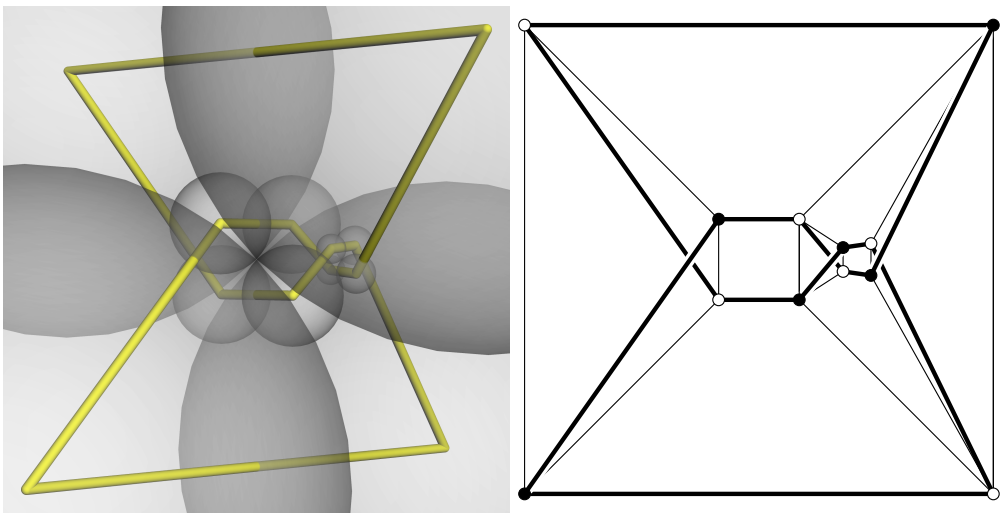

FIGURE 20. (Left) An orthocubic representation of the trefoil knot and its corresponding cubic diagram (right).

An orthocubic path will be encoded by a sequence of the orthocubic coordinates $[\![i_{w_1}, \cdots, i_{w_n}]\!]$ of the elements given in the linear order induced by γ. Since we shall consider unoriented paths, and the concatenation of two paths gives another path, vectors encoding orthocubic paths must be quotient by the following relations:

(i) (Symmetry) $[\![i_{w_1}, \cdots, i_{w_n}]\!] = [\![i_{w_n}, \ldots, i_{w_1}]\!]$.
(ii) (Concatenation) $\{[\![i_{w_1}, \cdots, i_{w_n}]\!], [\![i_{w_n}, \cdots, i_{w_m}]\!]\} = \{[\![i_{w_1}, \cdots, i_{w_n}, \cdots, i_{w_m}]\!]\}$.

4.4. **Orthocubic tangles.** Let $\mathcal{T}$ be the tetrahedron in the 3-skeleton of $\mathcal{B}_{\mathcal{O}^4}$ with vertices $\{\overline{1}, \overline{2}, 3, 4\}$. We define an *orthocubic tangle* as a tangle $(\mathcal{T}, \boxed{t})$ where $\boxed{t}$ is a collection $\{\gamma_1, \gamma_2, \ldots, \gamma_m\}$ of $m \geq 2$ disjoint orthocubic paths contained in $\mathcal{T}$ satisfying that the endpoints of γ_1 and γ_2 lie in the corners of $\mathcal{T}$, and the rest of the orthocubic paths are closed. In what follows, we construct the respective analog of the elementary tangles, sum, mirror, flip and half-twists for orthocubic tangles by using elements of the symmetrized Apollonian group of $\mathcal{B}_{\mathcal{O}^4}$.

(i) The *orthocubic elementary tangles*: $\boxed{t_0} := \{[\![\overline{1}, 4]\!], [\![3, \overline{2}]\!]\}$, $\boxed{t_1} := \{[\![\overline{1}, \overline{2}]\!], [\![3, 4]\!]\}$ and $\boxed{t_\infty} := \{[\![\overline{1}, 3]\!], [\![\overline{2}, 4]\!]\}$.

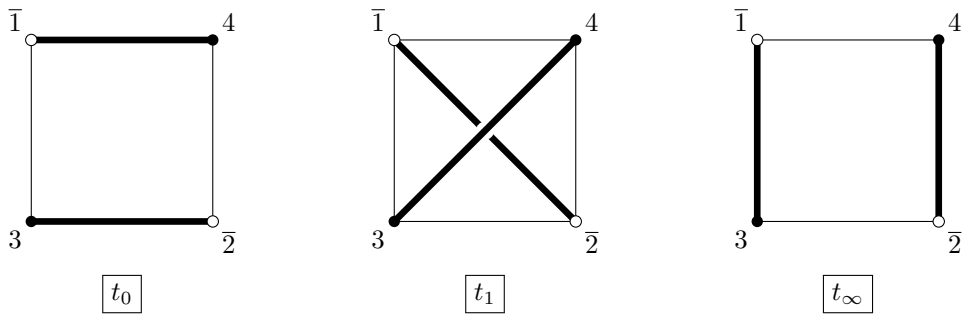

FIGURE 21. The elementary orthocubic tangles.

(ii) The *orthocubic flip* $F_{\mathcal{O}}\boxed{t} := r_{12}\boxed{t}$, where $r_{12} \in \mathsf{Sym}(\mathcal{B}_{\mathcal{O}^4})$ acting as the reflection on the plane $\{y = x\}$ in $\mathbb{R}^3$.
(iii) The *orthocubic mirror* $-\boxed{t} := \phi(\mu_{-3})\boxed{t} \cup \{[\![1, \overline{2}]\!], [\![\overline{1}, 2]\!], [\![3, \overline{4}]\!], [\![\overline{3}, 4]\!]\}$.

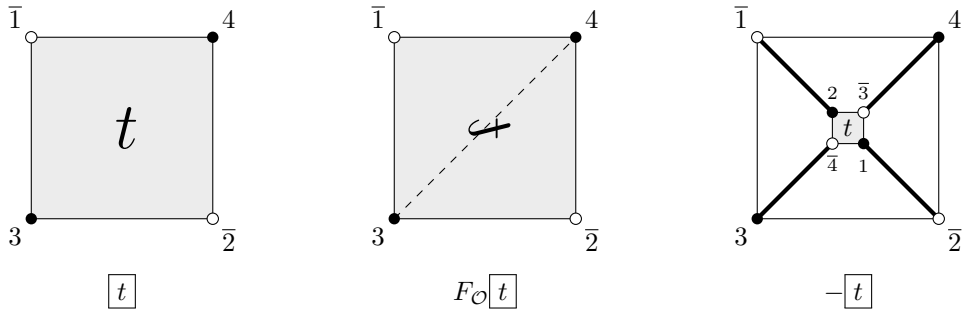

FIGURE 22. The orthocubic flip and mirror.

(iv) The orthocubic sum $\boxed{t'} + \boxed{t} := \phi(\mu_{-1})\boxed{t'} \cup \{[\![1, \overline{4}]\!], [\![2, \overline{3}]\!]\} \cup \phi(\mu_1)\boxed{t}$.
(v) The orthocubic half-twists $H^+_{\mathcal{O}}\boxed{t} := \boxed{t_1} + \boxed{t}$ and $H^-\boxed{t} := -\boxed{t_1} + \boxed{t}$.

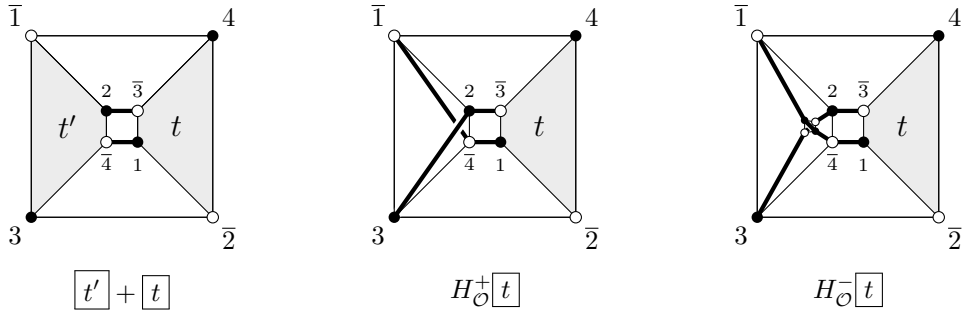

FIGURE 23. The orthocubic sum and half-twists.

We define the orthocubic *tangle closures* by:

(vi) The orthocubic numerator $N_{\mathcal{O}}\boxed{t} := \boxed{t} \cup \{[\![\overline{1}, 2_3, \overline{3}_3, 4]\!], [\![\overline{2}, 1_3, \overline{4}_3, 3]\!]\}$

(vi) The orthocubic denominator $D_{\mathcal{O}}\boxed{t} := \boxed{t} \cup \{[\![\overline{1}, 2_3, \overline{4}_3, 3]\!], [\![\overline{2}, 1_3, \overline{3}_3, 4]\!]\}$

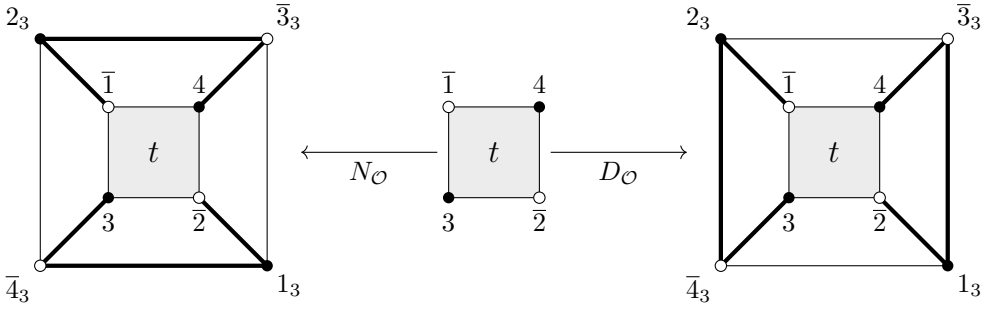

FIGURE 24. The orthocubic tangle closures.

Since the orthocubic elementary tangles, operations and closures are isotopically equivalent to their homonym in the classic framework of tangles, we can mimic the Conway's method to define an *orthocubic* rational tangle $t_{\mathcal{O}}[a_1, \cdots, a_n] \simeq t[a_1, \cdots, a_n]$, by

$$t_{\mathcal{O}}[a_1, \cdots, a_n] := H^{a_1}_{\mathcal{O}} F_{\mathcal{O}} \cdots H^{a_n}_{\mathcal{O}} F_{\mathcal{O}} \boxed{t_\infty} \tag{9}$$

We have now all the elements to prove the Theorem 4.1.

Proof of Theorem 4.1. Every rational tangle admits a necklace representation in $\mathscr{S}(\mathcal{B}_{\mathcal{O}^4})$, via the orthocubic version of Conway's construction. By combining the latter with the orthocubic tangle operations we obtain that any algebraic link admits an orthocubic representation. □

4.5. **Improvement of the upper bound of the ball number.** The orthocubic Conway's algorithm can be slightly adapted in order to improve the get the upper bound of Theorem 4.2. For every $a_1 \geq 0$, $a_2, \ldots, a_n > 0$, we define the *reduced* orthocubic Conway's algorithm $\widetilde{t}_{\mathcal{O}}[a_1, \cdots, a_n]$ by

$$\widetilde{t}_{\mathcal{O}}[a_1, \cdots, a_n] := H^{a_1}_{\mathcal{O}} F_{\mathcal{O}} \cdots H^{a_n - 1}_{\mathcal{O}} \boxed{t_1} \tag{10}$$

Clearly, for every $a_1 \geq 0$, $a_2, \ldots, a_n > 0$, we have $t_{\mathcal{O}}[a_1, \cdots, a_n] \simeq \widetilde{t}_{\mathcal{O}}[a_1, \cdots, a_n]$.

Theorem 4.2. *Let L be an algebraic link obtained by the closure of the algebraic tangle*

$$t_{p_1/q_1} + \cdots + t_{p_m/q_m}$$

where all the p_i/q_i have same sign. Then, $\mathsf{ball}(L) \leq 4\mathsf{cr}(L)$.

Proof. Let L be an algebraic link made by the closure $N(t)$ where t is the algebraic tangle

$$t_{p_1/q_1} + \cdots + t_{p_m/q_m}.$$

The condition that all p_i/q_i have the same sign implies that we have alternating diagram of L induced by the closure of t, and thus, by the Tait conjecture on the crossing number of alternating diagrams [Kau87; Thi87; Mur87], the crossing number of L is equal to the sum of the crossing numbers of each

t_{p_i/q_i}. Without loss of generality, we can consider that all p_i/q_i are positive. For every p_i/q_i with positive continued fraction $[a_1, \cdots, a_n]$, let $\boxed{t_{p_i/q_i}} := \widetilde{t}_{\mathcal{O}}[a_1, \cdots, a_n]$. Since the $F_{\mathcal{O}}$ does not change the necklace length, and $H^+_{\mathcal{O}}$ increases the necklace length by 4, we have that

$$\begin{aligned} |\boxed{t_{p_i/q_i}}| &= 4(a_1 + \ldots + a_n - 1) + |\boxed{t_1}| \\ &= 4(a_1 + \ldots + a_n) = 4\mathsf{cr}(t_{p_i/q_i}) \end{aligned}$$

Let $\boxed{t}$ be the orthocubic tangle made by the orthocubic sums $\boxed{t_{p_1/q_1}} + \cdots + \boxed{t_{p_m/q_m}}$. By the equivalence between the orthocubic and tangle operations we have that $\boxed{t} \simeq t$. Since the necklace length is additive for the sum,

$$\begin{aligned} |\boxed{t}| &= |\boxed{t_{p_1/q_1}}| + \cdots + |\boxed{t_{p_m/q_m}}| \\ &= 4\mathsf{cr}(t_{p_1/q_1}) + \cdots + 4\mathsf{cr}(t_{p_m/q_m}) \\ &= 4\mathsf{cr}(L). \end{aligned}$$

Finally, we notice that the exterior orthocubic paths $[\![\overline{1}, 4]\!]$ and $[\![\overline{2}, 3]\!]$ are not included in any orthocubic tangle obtained after applying an orthocubic sum. Therefore, we can use the exterior paths to close $\boxed{t}$, and in this way obtain a necklace representation of L with $4\mathsf{cr}(L)$ spheres. □

4.6. **No tightness for non-alternating links.** The family of algebraic links considered in Theorem 4.2 contains all the rational links and other well-known families as the *Montesinos links* with positive coefficients. These are the links obtained by the closure of

$$t_{p_1/q_1} + \cdots + t_{p_n/q_n} + t_r$$

with $p_i/q_i > 0$ and $r \geq 0$. If $r = 0$ and every $p_i = 1$, then we obtain the *Pretzel link* $P(q_1, \ldots, q_n)$.

In the non-alternating case, it is possible to construct orthocubic algebraic tangles with necklace length strictly less than 4 times the crossing number. The first non-trivial example that we have found satisfying this property, is the Pretzel knot $P(3, -2, 3)$, which corresponds to the knot 8_{19} in the Alexander-Briggs-Rolfsen notation. This knot is not alternating [Cro04] and it admits an orthocubic necklace representation with 28 spheres ($= \frac{3}{2}\mathsf{cr}(8_{19})$, see Figure 25). However, it becomes more tricky to establish a relation with the crossing number in the non-alternating case since, in general, the crossing number does not correspond to the sum of the crossings of its rational factors.

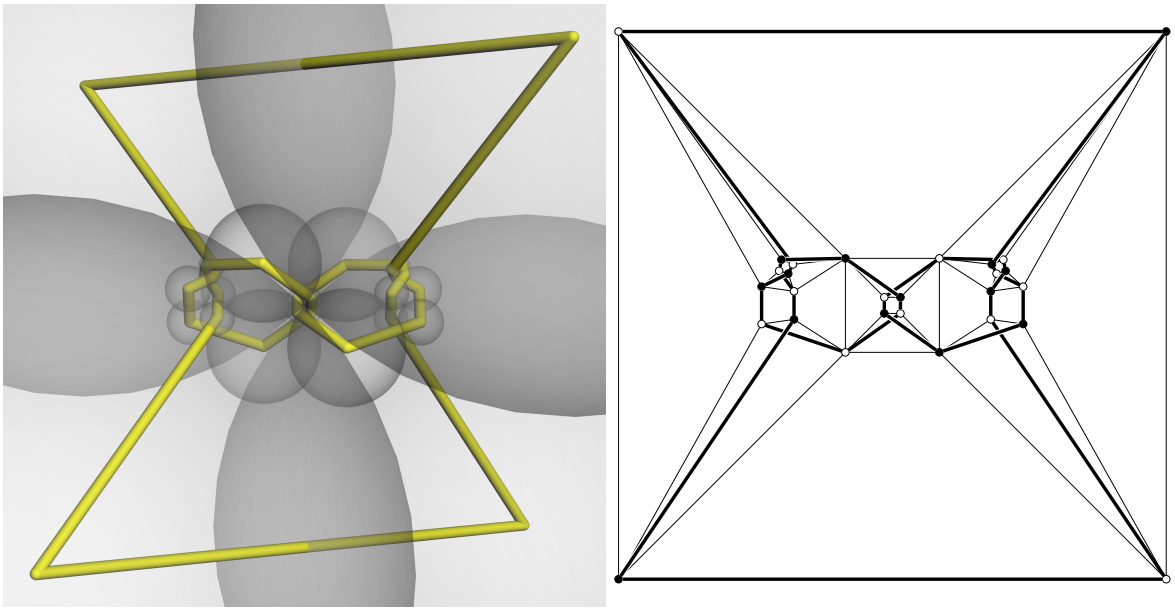

FIGURE 25. An orthocubic representation of the knot 8_{19} with 28 spheres (left) and its cubic diagram (right).

5. A new visualization of the slope of rational tangles

The slope p/q of a rational tangle $t_{p/q}$ can be identified with the slope of the meridian of a solid torus that is the branched double covering of a rational tangle [Cro04]. We shall present a new geometric interpretation of the correspondance between rational tangles and rational numbers. We do so by relating the slope of a tangle with the slope of the line passing through the origin and the last tangency point in the orthocubic Conway's construction. Astonishingly, this approach turns out to be helpful to find infinitely many primitive solutions of the Diophantine equation $x^4 + y^4 + z^4 = 2t^2$.

Let p/q be a positive fraction with positive continued fraction expansion $[a_1, \cdots, a_n]$. We define the *orthocubic point* $\eta_{p/q}$ of the rational tangle $t_{p/q}$ as the tangency point of the two disks in the cubic diagram of $t_{\mathcal{O}}(a_1, \cdots, a_n)$ corresponding to the *last edge* of the orthocubic tangle. By *last edge*, we mean the edge connecting the disk in the upper-right corner (see Figure 26). We point out that the disk in the upper-right corner corresponds to the sphere $b_{123} \in \mathcal{B}_{\mathcal{C}^3}$ which remains fixed under the orthocubic Conway's algorithm. We can naturally extend the notion of orthocubic point to tangles with negative fractions, by applying a reflection through the plane $\{x = 0\}$ to the whole setting.

Theorem 5.1. *For every $p/q \in \mathbb{Q}^{\pm} \cup \{\infty\}$, $\eta_{p/q}$ is the first intersection of the line passing through the origin and having slope $\pm(p/q)^{-2}$, with the boundary of the disk $b_{\pm 123} \in \mathcal{B}_{\mathcal{C}^3}$.*

Proof. It is enough to prove the positive case. Let $p \geq 0$ and $q \geq 1$ be two coprime integers. We claim that

$$\mathbf{i}(\eta_{p/q}) = \begin{pmatrix} p^2 \\ q^2 \\ (p-q)^2 \\ \sqrt{2}(p^2 - pq + q^2) \end{pmatrix}. \tag{11}$$

This would imply that the Cartesian coordinates of $\eta_{p/q}$ are

$$\frac{1}{\sqrt{2}pq - (1-\sqrt{2})(p-q)^2}(p^2, q^2),$$

which is exactly the first point of intersection of the line $\{p^2 y = q^2 x\}$ and the circle centred at $(1+\sqrt{2}, 1+\sqrt{2})$ and radius $(1+\sqrt{2})$, which is the boundary of $b_{123} \in \mathcal{B}_{\mathcal{C}^3}$.

Let us prove the equality (11). The positiveness of p and q implies that we can find a positive continued fraction expansion $[a_1, \cdots, a_n] = p/q$ with $a_1 \geq 0$ and $a_i \geq 1$ for every $1 < i \leq n$. Let $\boxed{t_{p/q}}$ the orthocubic tangle $t_{\mathcal{O}}[a_1, \ldots, a_n]$. Let $\eta_{p/q}$ and η_∞ be the orthocubic points of $t_{p/q}$ and t_∞, respectively. Now, by the definitions of the orthocubic operations $H_{\mathcal{O}}$ and $F_{\mathcal{O}}$, the isomorphism $\phi : \mathsf{SA}(\mathcal{B}_{\mathcal{C}^3}) \longrightarrow \mathsf{SA}(\mathcal{B}_{\mathcal{O}^4})$ and the definition of orthocubic rational tangles given in (9), we have that

$$\begin{aligned} \boxed{t_{p/q}} = H_{\mathcal{O}}^{a_1} F_{\mathcal{O}} \cdots H_{\mathcal{O}}^{a_n} F_{\mathcal{O}} \boxed{t_\infty} \Rightarrow \eta_{p/q} &= \mu_1^{a_1} r_{12} \cdots \mu_x^{a_n} r_{12}(\eta_\infty) \\ &= (s_1 r_{13})^{a_1} r_{12} \cdots (s_1 r_{13})^{a_n} r_{12}(\eta_\infty) \end{aligned}$$

where s_1, r_{13} and r_{12} are the elements of $\mathsf{SA}(\mathcal{B}_{\mathcal{C}^3})$ described in subsection 4.1. The inversive coordinates of η_∞ and the matrices representing s_1, r_{13} and r_{12} can be computed by using the equations (2) (with $\lambda = \frac{1+\sqrt{2}}{2}$) and (4), giving

$$\mathbf{i}(\eta_\infty) = \begin{pmatrix} 1 \\ 0 \\ 1 \\ \sqrt{2} \end{pmatrix}, \qquad s_1 \mapsto \mathbf{S}_1 = \begin{pmatrix} -3 & 0 & 0 & 2\sqrt{2} \\ 0 & 1 & 0 & 0 \\ 0 & 0 & 1 & 0 \\ -2\sqrt{2} & 0 & 0 & 3 \end{pmatrix},$$

$$r_{13} \mapsto \mathbf{R}_{13} = \begin{pmatrix} 0 & 0 & 1 & 0 \\ 0 & 1 & 0 & 0 \\ 1 & 0 & 0 & 0 \\ 0 & 0 & 0 & 1 \end{pmatrix}, \quad r_{12} \mapsto \mathbf{R}_{12} = \begin{pmatrix} 0 & 1 & 0 & 0 \\ 1 & 0 & 0 & 0 \\ 0 & 0 & 1 & 0 \\ 0 & 0 & 0 & 1 \end{pmatrix}.$$

Let $\mathbf{M}(k) := (\mathbf{S}_1\mathbf{R}_{13})^k\mathbf{R}_{12}$. By induction on k, it can be found that

$$\mathbf{M}(k) = \begin{pmatrix} 0 & 1-k^2 & -k(k+2) & \sqrt{2}k(k+1) \\ 1 & 0 & 0 & 0 \\ 0 & -k(k-2) & 1-k^2 & \sqrt{2}k(k-1) \\ 0 & -\sqrt{2}k(k-1) & -\sqrt{2}k(k+1) & 2k^2+1 \end{pmatrix}$$

We will finally prove the equality (11) by induction on the number of coefficients n in the fraction expansion of p/q. For $n = 1$ (that is $p = a_1$ and $q = 1$) we have

$$\mathbf{i}(\eta_{a_1}) = \mathbf{M}(a_1)\begin{pmatrix} 1 \\ 0 \\ 1 \\ \sqrt{2} \end{pmatrix} = \begin{pmatrix} a_1^2 \\ 1 \\ (a_1-1)^2 \\ \sqrt{2}(a_1^2-a_1+1) \end{pmatrix}.$$

We suppose equality (11) to be true for $n-1 \geq 1$. Let $r/s = a_2 + \frac{1}{\cdots+\frac{1}{a_n}}$. Then,

$$\begin{aligned} \mathbf{i}(\eta_{p/q}) = \mathbf{M}(a_1)\mathbf{M}(a_2)\cdots\mathbf{M}(a_n)\begin{pmatrix} 1 \\ 0 \\ 1 \\ \sqrt{2} \end{pmatrix} &= \mathbf{M}(a_1)\begin{pmatrix} r^2 \\ s^2 \\ (r-s)^2 \\ \sqrt{2}(r^2-rs+s) \end{pmatrix} \\ &= \begin{pmatrix} (ra_1+s)^2 \\ r^2 \\ (ra_1+s-r)^2 \\ \sqrt{2}((ra_1+s)^2-r(ra_1+s)+r^2) \end{pmatrix} \end{aligned}$$

We finally notice that

$$\frac{ra_1+s}{r} = a_1 + \frac{s}{r} = a_1 + \frac{1}{r/s} = a_1 + \frac{1}{a_2 + \frac{1}{\cdots+\frac{1}{a_n}}} = \frac{p}{q}$$

and therefore, equality (11) holds. □

Corollary 5.1. *The Diophantine equation*

$$x^4 + y^4 + z^4 = 2t^2 \tag{12}$$

has an infinite number of primitive solutions.

Proof. Since points of $\widehat{\mathbb{R}^2}$ correspond to light-like vectors of $\mathbb{L}^{3,1}$, we can use the inversive coordinates of the orthocubic point of every rational tangle given in equation (11) to produce primitive solutions of the Diophantine equation by taking

$$x = p, \qquad y = q, \qquad z = p - q, \qquad t = p^2 - pq + q^2. \tag{13}$$

□

We hope and expect the above approach to be helpful to investigate solutions of other type of Diophantine equations.

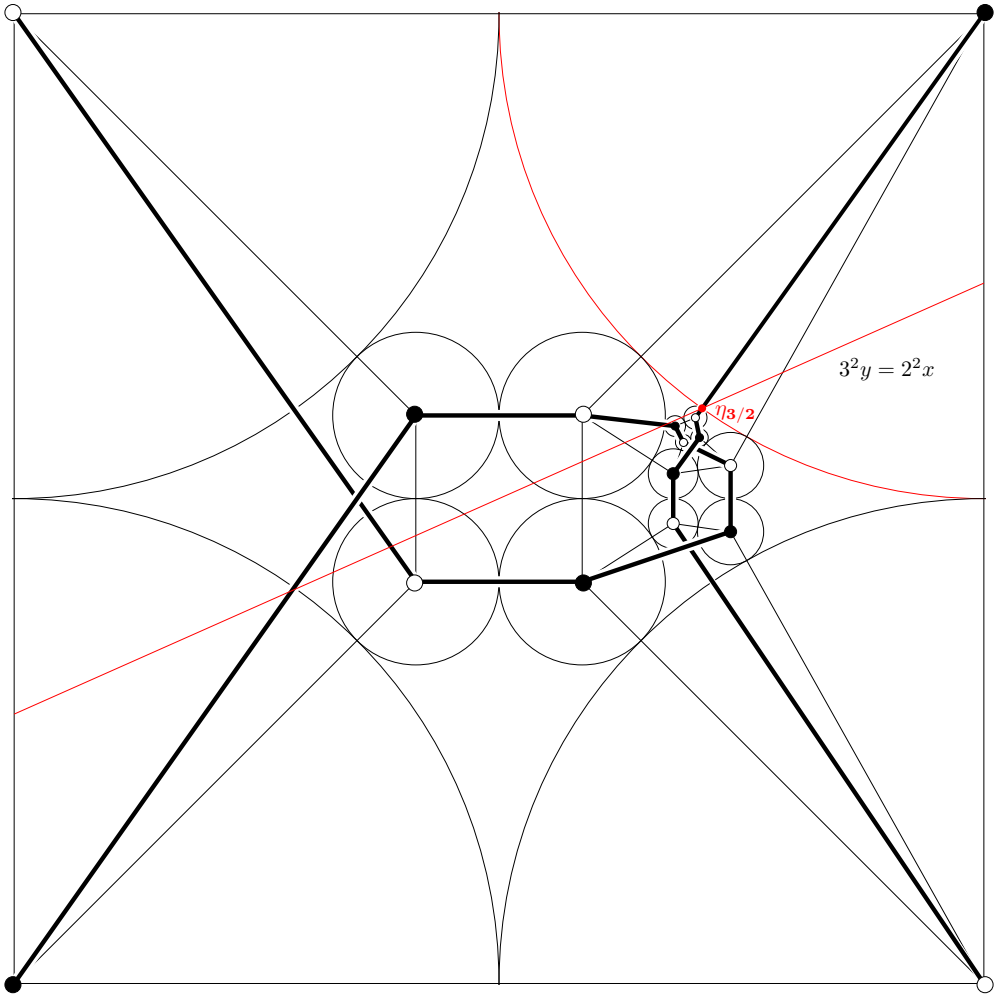

FIGURE 26. The orthocubic point (red) of the rational tangle $t_{3/2}$ corresponding to the primitive solution $3^4 + 2^4 + 1^4 = 2 \times 7^2$.

REFERENCES

[Ada94] C. C. Adams. *The knot book*. American Mathematical Soc., 1994.

[Ale23] J. W. Alexander. "A lemma on systems of knotted curves". In: *Proceedings of the National Academy of Sciences of the United States of America* 9.3 (1923), p. 93.

[AM95] S. V. Anishchik and N. N. Medvedev. "Three-Dimensional Apollonian Packing as a Model for Dense Granular Systems". In: *Phys. Rev. Lett.* 75 (23 1995), pp. 4314–4317. DOI: 10.1103/PhysRevLett.75.4314. URL: https://link.aps.org/doi/10.1103/PhysRevLett.75.4314.

[Con70] J. H. Conway. "An enumeration of knots and links, and some of their algebraic properties". In: *Computational problems in abstract algebra*. Elsevier. 1970, pp. 329–358.

[Cro04] P. R. Cromwell. *Knots and Links*. Cambridge University Press, 2004. DOI: 10.1017/CBO9780511809767.

[Epp14] D. Eppstein. "Links and knots in the graphs of four-dimensional polytopes". In: (2014). URL: https://11011110.github.io/blog/2014/12/13/links-and-knots.html.

[Gab+21] D. Gabai, R. Haraway, R. Meyerhoff, N. Thurston, and A. Yarmola. *Hyperbolic 3-manifolds of low cusp volume*. 2021. arXiv: 2109.14570 [math.GT].

[GT86] D. Gabai and W. P. Thurston. *Genera of Arborescent Links: 1986*. Vol. 339. American Mathematical Soc., 1986.

[Gra+03] R. Graham, J. C. Lagarias, C. L. Mallows, A. R. Wilks, and C. H. Yan. "Apollonian circle packings: number theory". In: *Journal of Number Theory* 100.1 (2003), pp. 1–45. ISSN: 0022-314X. DOI: https://doi.org/10.1016/S0022-314X(03)00015-5. URL: https://www.sciencedirect.com/science/article/pii/S0022314X03000155.

[Kau87] L. H. Kauffman. "State models and the Jones polynomial". In: *Topology* 26.3 (1987), pp. 395–407.

[KN19] A. Kontorovich and K. Nakamura. "Geometry and arithmetic of crystallographic sphere packings". In: *Proceedings of the National Academy of Sciences* 116.2 (2019), pp. 436–441. ISSN: 0027-8424. DOI: 10.1073/pnas.1721104116. eprint: https://www.pnas.org/content/116/2/436.full.pdf. URL: https://www.pnas.org/content/116/2/436.

[Kwo+20] S. Kwok, R. Botet, L. Sharpnack, and B. Cabane. "Apollonian packing in polydisperse emulsions". In: *Soft Matter* 16 (10 2020), pp. 2426–2430. DOI: 10.1039/C9SM01772K. URL: http://dx.doi.org/10.1039/C9SM01772K.

[Mae07] H. Maehara. "On Configurations of Solid Balls in 3-Space: Chromatic Numbers and Knotted Cycles". In: *Graphs and Combinatorics* 23.1 (2007), pp. 307–320. ISSN: 1435-5914. DOI: 10.1007/s00373-007-0702-7. URL: https://doi.org/10.1007/s00373-007-0702-7.

[Mur87] K. Murasugi. "Jones polynomials and classical conjectures in knot theory". In: *Topology* 26.2 (1987), pp. 187–194.

[Nak14] K. Nakamura. *The local-global principle for integral bends in orthoplicial Apollonian sphere packings*. 2014. arXiv: 1401.2980 [math.NT].

[RR21a] J. L. Ramírez Alfonsín and I. Rasskin. "A polytopal generalization of Apollonian packings and Descartes' theorem". In: (2021). arXiv: 2107.09432 [math.CO].

[RR21b] J. L. Ramírez Alfonsín and I. Rasskin. "Ball packings for links". In: *European Journal of Combinatorics* 96 (2021), p. 103351. ISSN: 0195-6698. DOI: https://doi.org/10.1016/j.ejc.2021.103351. URL: https://www.sciencedirect.com/science/article/pii/S0195669821000433.

[Ras21] I. Rasskin. "Regular polytopes, sphere packings and Apollonian sections". In: *arXiv preprint arXiv:2109.00655* (2021).

[Sta15] K. E. Stange. "The Apollonian structure of Bianchi groups". In: *Transactions of the American Mathematical Society* 370 (May 2015). DOI: 10.1090/tran/7111.

[Ste05] K. Stephenson. *Introduction to circle packing: The theory of discrete analytic functions*. Cambridge University Press, 2005.

[Thi87] M. B. Thistlethwaite. "A spanning tree expansion of the Jones polynomial". In: *Topology* 26.3 (1987), pp. 297–309.

[Wil81] J. B. Wilker. "Inversive Geometry". In: (1981). Ed. by Chandler Davis, Branko Grünbaum, and F. A. Sherk, pp. 379–442.

IMAG, Univ. Montpellier, CNRS, Montpellier, France
Email address: jorge.ramirez-alfonsin@umontpellier.fr

Institute of Analysis and Number Theory, TU Graz, Austria
Email address: ivan.rasskin@math.tugraz.at